Experiment and Modeling of CO2 Capture from Flue Gases at High Temperature in a Fluidized Bed Reactor with Ca-Based Sorbents

ARTICLE *in* ENERGY & FUELS · DECEMBER 2008

Impact Factor: 2.79 · DOI: 10.1021/ef800474n

3 AUTHORS, INCLUDING:

Ningsheng Cai
Tsinghua University
138 PUBLICATIONS **1,793** CITATIONS

SEE PROFILE

Experiment and Modeling of CO_2 Capture from Flue Gases at High Temperature in a Fluidized Bed Reactor with Ca-Based Sorbents

Fan Fang, Zhen-Shan Li, and Ning-Sheng Cai*

Key Laboratory for Thermal Science and Power Engineering of the Ministry of Education (MOE), Department of Thermal Engineering, Tsinghua University, Beijing 100084, China

Received June 17, 2008. Revised Manuscript Received October 31, 2008

The cyclic CO_2 capture and $CaCO_3$ regeneration characteristics in a small fluidized bed reactor were experimentally investigated with limestone and dolomite sorbents. Kinetic rate constants for carbonation and calcination were determined using thermogravimetric analysis (TGA) data. Mathematical models developed to model the Ca-based sorbent multiple cycles of CO_2 capture and calcination in the bubbling fluidized bed reactor agreed with the experimental data. The experimental and simulated results showed that the CO_2 in flue gases could be absorbed efficiently by limestone and dolomite. The time for high-efficiency CO_2 capture decreased with an increasing number of cycles because of the loss of sorbent activity, and the final CO_2 capture efficiency remained nearly constant as the sorbent reached its final residual capture capacity. In a continuous carbonation and calcination system, corresponding to the sorbent activity loss, the carbonation kinetic rates of sorbent undergoing various cycles are different, and the carbonation kinetic rates of sorbent circulating N times in the carbonation/calcination cycles are also different because of the different residence time of sorbent in the carbonator. Therefore, the average carbonation rate was given based on the mass balance and exit age distribution for sorbent in the carbonator. The CO_2 capture characteristics in a continuous carbonation/calcination system were predicted, taking into consideration the mass balance, sorbent circulation rate, sorbent activity loss, and average carbonation kinetic rate, to give useful information for the reactor design and operation of multiple carbonation/calcination reaction cycles.

1. Introduction

The environmental impact of anthropogenic CO_2 emissions is now recognized to be the major risk to mankind, because the CO_2 emissions into the atmosphere have been reported to account for half of the greenhouse effect, which causes global warming.[1] Therefore, reducing the CO_2 emissions will be the greatest industrial challenge of the 21st century. CO_2 (or carbon) capture and storage (CCS) has the potential to make a significant contribution to reduce CO_2 released from large point sources. CCS processes aim to reduce CO_2 emissions by capturing CO_2 from industrial (power, cement, and steel) processes that burn fossil fuels and storing the CO_2 in deep saline aquifers, depleted oil/gas fields, deep coal seams, or deep ocean reservoirs to allow for the continued use of coal, oil, and gas while avoiding the CO_2 emissions currently associated with fossil fuel use. The estimated costs for CO_2 transport (U.S. \$1−3 per ton per 100 km)[2] and sequestration (U.S. \$4−8 per ton of CO_2)[3] are small compared to the cost for CO_2 capture, estimated at U.S. \$35−55 per ton of CO_2 captured.[4] Therefore, reducing the cost of CO_2 capture is the absolute focus of attention to make CCS more economically attractive.

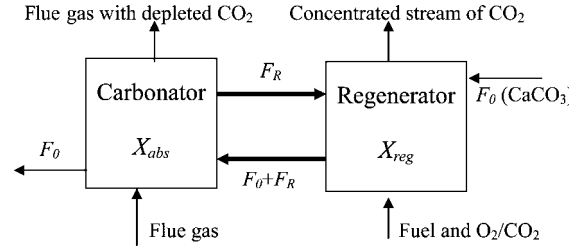

Figure 1. Schematic of carbonation/calcination cycle using Ca-based sorbents.

There are various approaches to separate CO_2 from flue gas streams. This paper focuses on the use of the multiple carbonation/calcination reaction (CCR) cycles with Ca-based sorbents as shown in Figure 1. The carbonation reaction of lime (CaO) with CO_2 and its reverse reaction have been proposed by many researchers to separate CO_2 from gaseous mixtures.[5−9] The overall system of the CCR process consists of a carbonation reactor and a calcination reactor. In the carbonator, CaO is carbonated to $CaCO_3$ at a relatively low temperature in the flue gas (about 600−700 °C) at atmospheric pressure

* To whom correspondence should be addressed. Telephone: +86-10-62789955. Fax: +86-10-62770209. E-mail: cains@tsinghua.edu.cn.

(1) Houghton, J. T. *Climate Change 1995: The Science of Climate Change, Contribution of Working Group I to the Second Assessment Report of the Intergovernmental Panel on Climate Change*; Cambridge University Press: Cambridge, U.K., 1996.
(2) Freund, P. *Proc. Inst. Mech. Eng.* **2003**, *217* (1), 1–7.
(3) Lyngfelt, A.; Leckner, B.; Mattisson, T. *Chem. Eng. Sci.* **2001**, *56* (10), 3101–3113.
(4) Singh, D.; Croiset, E.; Douglas, P. L.; Douglas, M. A. *Energy Convers. Manage.* **2003**, *44* (19), 3073–3091.
(5) Shimizu, T.; Hirama, T.; Hosoda, H.; Kitano, K.; Inagaki, M.; Tejima, K. *Trans. IChemE* **1999**, *77*, 62–68.
(6) Balasubramanian, B.; Lopez, O. A.; Kaytakoglu, S.; Harrison, D. P. *Chem. Eng. Sci.* **1999**, *54* (15−16), 3543–3552.
(7) Hughes, R. W.; Lu, D. Y.; Anthony, E. J.; Macchi, A. *Fuel Process. Technol.* **2005**, *86* (14), 1523–1531.
(8) Gupta, H.; Fan, L. S. *Ind. Eng. Chem. Res.* **2002**, *41* (16), 4035–4042.
(9) Abanades, J. C.; Anthony, E. J.; Wang, J. S.; Oakey, J. E. *Environ. Sci. Technol.* **2005**, *39*, 2861–2866.

10.1021/ef800474n CCC: \$40.75
Published on Web 12/23/2008

$$CaO(s) + CO_2(g) \rightarrow CaCO_3(s) \quad \Delta H_{298}{}^0 = -178 \text{ kJ/mol} \quad (1)$$

The $CaCO_3$ is then removed from the carbonator and delivered to the regenerator. The calcination of $CaCO_3$ regenerates the sorbent to CaO and produces a concentrated stream of CO_2 at higher temperatures (>900 °C). In practical applications, because the reaction of CaO and CO_2 (eq 1) is exothermic, steam can be produced by immersing heat-transfer surfaces in the carbonator. The calcination of $CaCO_3$ (eq 2) is an endothermic reaction, with the heat of reaction supplied by burning fuel with pure O_2 or O_2/CO_2 in the regenerator.

$$CaCO_3(s) \rightarrow CaO(s) + CO_2(g) \quad \Delta H_{298}{}^0 = 178 \text{ kJ/mol} \quad (2)$$

For continuous processes, the CO_2 sorbents must be regenerated after the carbonation reaction to be used repeatedly. Accordingly, the cyclic carbonation/regeneration characteristics of these sorbents are very important for practical applications. Naturally occurring Ca-based sorbents, such as limestone and dolomite, which are plentiful, cheap, and widely available, are suitable for the CO_2 separation process, but their CO_2 capture capacity decreases during multiple carbonation/calcination reaction cycles. Many previous studies[10−13] have investigated the multicycle performance of carbonation/calcination reactions of limestone and dolomite. These studies indicated that the maximum carbonation capacity decreased with the number of cycles because of the loss of a suitable pore volume in the sorbents and sintering between adjacent grains and that the dolomite had better cyclic carbonation capacity than limestone. However, most of these investigations were carried out using thermogravimetric analyzers, fixed bed reactors, or fluidized bed reactors operated under mild calcination conditions[14,15] (low CO_2 fractions and temperatures). For practical processes, using the carbonation/calcination cycles, the $CaCO_3$ must be regenerated in a rich CO_2 atmosphere (more than 90%) to obtain a relatively high-purity CO_2 stream. According to the thermodynamic equilibrium of CaO with CO_2[16] (eq 3), the equilibrium temperature (when carbonation and calcination are balanced and the Gibbs free-energy change is zero) increases with increasing CO_2 partial pressure. Accordingly, the regeneration condition should be a rich CO_2 atmosphere (more than 90%) and a high temperature (>900 °C). Therefore, the first objective of this study was to obtain experimental data on the carbonation/calcination cycles of limestone and dolomite in a fluidized bed reactor under relatively severe calcination conditions (CO_2 concentrations above 90%) and then to develop a mathematical model for both the multiple carbonation and calcination reactions in a fluidized bed reactor considering the temperature, heat transfer, and the number of cycles and to validate the model with the experimental data.

$$P_{e,CO_2} = 4.137 \times 10^7 \exp\left(-\frac{20474}{T}\right) \quad (3)$$

In the CCR processes, sorbent circulates between the carbonator and the regenerator and the dual fluidized bed reactors are considered to be a suitable system for this process. For this continuous process, the Ca-based sorbents experience a decrease in their capacity of capturing CO_2 during multiple carbonation/calcination cycles and the carbonation kinetic rates of the Ca-based sorbents also decrease with the number of cycles. These two changes are critical for the design and operating conditions of the dual fluidized bed system. Therefore, the second purpose of this study is to combine the developed model with the sorbent activity decrease, carbonation rate decrease, and mass balance between the carbonator and regenerator to predict the CO_2 capture and the carbonator height in a continuous carbonation/calcination system to give useful information for the design of the dual fluidized bed CO_2 capture system.

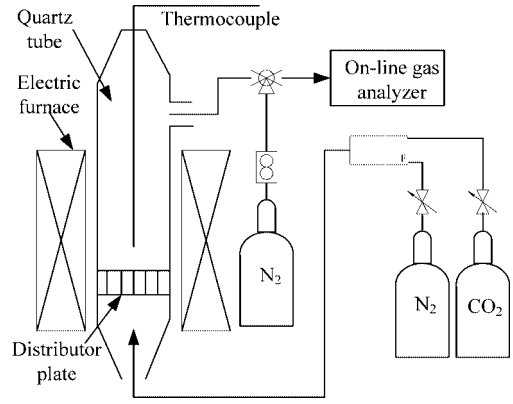

Figure 2. Experimental bubbling fluidized bed system.

2. Experimental Section

2.1. Carbonation and Calcination of Sorbent in a Thermogravimetric Analyzer (TGA). A Dupont 951 TGA (TA Instrument 1200) was used to study the carbonation and calcination characteristics of Ca-based CO_2 sorbents. The test system is described in detail by Li et al.[17] The following operating conditions were used for the carbonation/calcination tests: (i) the carbonation temperature was 650 °C, and the calcination temperature was 950 °C; (ii) the gas flow rate was 200 mL/min; (iii) the gas composition of CO_2/N_2 in the carbonation process was 20/80%, while it was 90/10% in the calcination; (iv) 200−450 μm limestone was used as the sorbent; (v) a three-way valve was used to switch between the carbonation gas mixture and the calcination gas mixture at the specified carbonation and calcination time intervals; and (vi) the carbonation time was 15 min, and the calcination time was 5 min.

2.2. Multicycle Tests of the Carbonation and Calcination Reactions in a Small Bubbling Fluidized Bed Reactor. The multicycle tests of the carbonation and calcination reactions were carried out in a small bubbling fluidized bed reactor (0.035 m i.d.). A schematic of the experimental bubbling fluidized bed system is presented in Figure 2. The flow rates of CO_2 and N_2 from high-purity cylinders were controlled by mass flow controllers. The combined feed gases entered near the bottom of the reactor and were preheated as they flowed upward. The preheated gas flowed upward through the sorbents, reacted with the sorbents, and exited at the top of the reactor. The thermocouple temperature measurements were recorded by a data acquisition system. The exit stream from the fluidized bed reactor was directly sampled at the reactor outlet by an online gas analyzer during the carbonation process. The online gas analyzer range for measuring CO_2 concentrations was 0−50%, and in the multicalcination processes, the CO_2 concentration at the exit of the small fluidized bed was higher than 90%; therefore, the exit gas from the reactor must be

(10) Li, Z.-S.; Cai, N.-S.; Huang, Y.-Y. *Ind. Eng. Chem. Res.* **2006**, *45*, 1911–1917.
(11) Li, Z.-S.; Cai, N.-S.; Huang, Y.-Y.; Han, H.-J. *Energy Fuels* **2005**, *19*, 1447–1452.
(12) Abanades, J. C.; Alvarez, D. *Energy Fuels* **2003**, *17*, 308–315.
(13) Abanades, J. C.; Anthony, E. J.; Lu, D. Y.; Salvador, C.; Alvarez, D. *AIChE J.* **2004**, *50* (7), 1614–1622.
(14) Ryu, H. J.; Grace, J. R.; Lim, C. J. *Energy Fuels* **2006**, *20* (4), 1621–1628.
(15) Salvador, C.; Lu, D.; Anthony, E. J.; Abanades, J. C. *Chem. Eng. J.* **2003**, *96*, 187–195.
(16) Silcox, G. D.; Kramlich, J. C.; Pershing, D. W. *Ind. Eng. Chem. Res.* **1989**, *28*, 155–160.
(17) Li, Z.-S.; Cai, N.-S. *Energy Fuels* **2007**, *21*, 2909–2918.

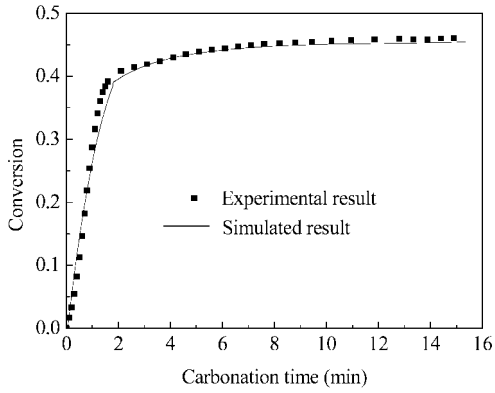

Figure 3. Conversion of CaO to $CaCO_3$ with time in the TGA at the temperature of 650 °C.

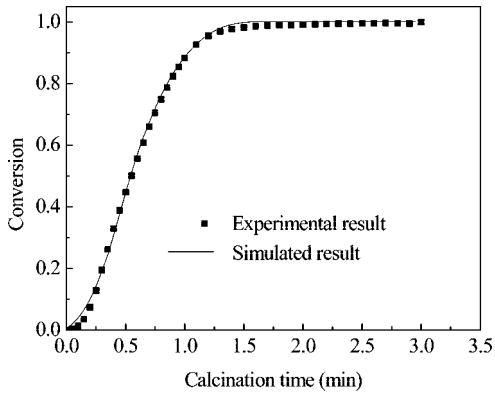

Figure 4. Conversion of $CaCO_3$ to CaO with time in the TGA.

diluted using additional pure N_2. Then, the CO_2 concentration in the combined gas was determined using the online gas analyzer and recorded by the data acquisition system. The temperatures for carbonation and calcination were ~650 and ~950 °C, respectively. The simulated flue gas contained ~16% bulk concentration CO_2 for all of the carbonation tests, with the rest being nitrogen. During the calcination stage, ~90% bulk concentration CO_2 (the rest was nitrogen) flowed through the reactor. Limestone and dolomite were used as CO_2 sorbents, both sieved to ensure that all of the particles were between 200 and 450 μm in size. The superficial gas velocity was between 0.06 and 0.09 m/s. A total of 80−100 g of sorbent was added into the reactor for each test.

3. Mathematical Model

3.1. Repeated Carbonation/Calcination Reactions of Ca-Based Sorbents in the Thermogravimetric Analysis. The variation of the carbonation conversion of lime with time from the TGA experiments is shown in Figure 3. Previous experimental results[17] indicated that the carbonation rate was independent of the temperature in the range of 600−700 °C and the ultimate conversion of CaO was independent of the CO_2 fraction in the carbonation process but increased as the reaction temperature increased. The previous experimental results[17] also showed that the CO_2 fraction had some effect on the carbonation rate with faster carbonation rates as the CO_2 fraction increases. Therefore, the CaO carbonation was expressed as a semi-empirical equation (eq 4), where C_{CO_2} is the CO_2 concentration in the gas phase. The precise conditions for the validity of this equation could be found in previous work.[17]

$$\frac{dX}{dt} = k_c\left(1 - \frac{X}{X_u}\right)^{2/3}(C_{CO_2} - C_{eq,CO_2})^{(P/P_0)^{0.083}} \quad (4)$$

The correction term $(P/P_0)^{0.083}$ accounts for the effect of the total pressure on the carbonation rate. In this work, the total pressure P is equal to the atmospheric pressure P_0. The reaction of CaO with CO_2 has two stages. The initial carbonation stage of CaO with CO_2 is fast and kinetically controlled. Then, the reaction slows and enters the product layer diffusion stage. A constant m is used to modify eq 4 to reflect these two stages in the semi-empirical equation (eq 5)

$$\frac{dX}{dt} = k_c\left(1 - \frac{X}{X_u}\right)^m(C_{CO_2} - C_{eq,CO_2}) \quad (5)$$

In eq 5, the value of m is $^2/_3$ for the kinetically controlled stage and $^4/_3$ for the product layer diffusion stage. k_c can be obtained from the experimental results. The predicted result for the CaO carbonation process is shown in Figure 3, with k_c = 0.0021 for the kinetically controlled stage and k_c = 0.0025 for the product layer diffusion stage. This apparent kinetic expression for the CaO carbonation was extended to multiple carbonation/calcination cycles as

$$\frac{dX_N}{dt} = k_c\left(1 - \frac{X_N}{X_{u,N}}\right)^m(C_{CO_2} - C_{eq,CO_2}) \quad (6)$$

In eq 6, X_N and $X_{u,N}$ denote the fractional conversion of CaO to $CaCO_3$ in the Nth cycle and the ultimate conversion of CaO in the Nth cycle, respectively.

The carbonation was tested at 650 °C for 15 min with the flow of CO_2 and N_2 into the TGA changing to the new ratio (90/10%), and the temperature increased from 650 to 950 °C and was kept for 5 min for the calcination period. The calcination conversion of limestone with time in the atmospheric pressure is shown in Figure 4. The temperature and CO_2 concentration inhibited the reaction rate of $CaCO_3$ to CaO. The apparent kinetic model for the conversion rate of $CaCO_3$ to CaO can be expressed as

$$\frac{dX_{calci}}{dt} = k_{calci}(1 - X_{calci})^{2/3}(C_{eq,CO_2} - C_{CO_2}) \quad (7)$$

The chemical reaction rate constant for the $CaCO_3$ calcination process is[17]

$$k_{calci} = k_{0,calci}\exp\left(-\frac{150000}{RT}\right) \quad (8)$$

The predicted $CaCO_3$ calcination shown in Figure 4 fits the experimental results well when $k_{0,calci}$ = 23 797.

3.2. Repeated Carbonation/Calcination Reactions of Ca-Based Sorbents in the Fluidized Bed Reactor. The fluidization conditions (u_0 = 0.6−0.9 m/s) and particle sizes of limestone and dolomite (0.2−0.45 mm) used in this study were in the range of intermediate regime between the extremes of very fast and slow bubbles.[18] The bubbling fluidized bed model (KL model)[18] was adapted to describe the experimental phenomenon. It considered that there were two regions, bubble and emulsion, in a bubbling fluidized bed, with just one interchange coefficient, K_{be}, to represent the transfer of gas between these two regions. On the basis of the KL model, the CO_2 axial concentration profile in the bubble, C_{b,CO_2}, and in the emulsion, C_{e,CO_2}, as a function of bed height, z, are given by

$$-\delta u_b^* \frac{dC_{b,CO_2}}{dz} = \delta K_{be}(C_{b,CO_2} - C_{e,CO_2}) + \delta\gamma_b f_a K_r(C_{b,CO_2} - C_{eq,CO_2}) \quad (9)$$

and

$$-(1-\delta)u_{mf}\frac{dC_{e,CO_2}}{dz}=(1-\delta)(1-\varepsilon_{mf})f_aK_r(C_{e,CO_2}-C_{eq,CO_2})-\delta K_{be}(C_{b,CO_2}-C_{e,CO_2}) \quad (10)$$

In these expressions, K_r is the reaction rate constant and C_{eq,CO_2} is the equilibrium CO_2 concentration over CaO, which for the temperature interval interest was given by Baker[19]

$$C_{eq,CO_2}=\frac{1.462\times10^{11}}{T}\exp(-19130/T) \quad (11)$$

γ_b is the void fraction of solids dispersed in the bubbles. From the experiment data, γ_b was about $10^{-2}-10^{-3}$, with the actual value uncertain.[20] $\gamma_b = 0.005$ was used as the void fraction of solids dispersed in the bubbles in the calculations.

K_{be} is the overall gas interchange coefficient between the bubble and emulsion phases given by Kunii and Levenspiel[18]

$$K_{be}=4.5\frac{u_{mf}}{d_b} \quad (12)$$

where u_{mf} is the superficial gas velocity at the minimum fluidizing conditions given by

$$u_{mf}=\frac{d_p{}^2(\rho_s-\rho_g)g}{150\mu}\frac{\varepsilon_{mf}{}^3\phi_s{}^2}{1-\varepsilon_{mf}} \quad (13)$$

where ε_{mf} is the void fraction in the bed at the minimum fluidizing conditions and ϕ_s is the sphericity of the sorbent particle, with $\varepsilon_{mf} = 0.5$ and $\phi_s = 0.67$ used here. d_b is the bubble diameter, assumed to be 0.02 m. A value proportional to the extreme is adopted to estimate the bubble fraction for the bubbling regime

$$\delta=\frac{u_0-u_{mf}}{u_b+\dfrac{5u_{mf}-u_b\varepsilon_{mf}}{4}} \quad \text{for } 1<\frac{u_b\varepsilon_{mf}}{u_{mf}}<5 \quad (14)$$

where u_b is a bubble rising velocity through the bed

$$u_b=u_0-u_{mf}+0.711(gd_b)^{0.5} \quad (15)$$

The rise velocity of the bubble gas, u_b^*, is calculated from the superficial gas velocity, u_0, the bubble fraction, δ, and the minimum fluidizing velocity, u_{mf}, from the gas balance in a bed cross-section

$$u_b^*=\frac{u_0-(1-\delta)u_{mf}}{\delta} \quad (16)$$

At any time in the multicarbonation experiments, the bed contains three types of solids: a fraction of CaO reacting in the fast reaction regime, a fraction of inactive CaO from previous carbonation/calcination cycles, and a fraction of $CaCO_3$.[13] Therefore, f_a was defined as the fraction of active CaO in the carbonation process. While in the multicalcination experiments, the sorbents consisted of two kinds of solids: CaO and $CaCO_3$. f_a was then defined as the fraction of nonreacting $CaCO_3$ to the sorbent in the calcination process

$$f_a=X_{u,N}-X_N \quad \text{for the carbonation stage} \quad (17)$$

$$f_a=(1-X_{calci})X_{u,N} \quad \text{for the calcination stage} \quad (18)$$

The energy balance for the carbonation process with limestone can be written as

$$\frac{W_0}{M_{CaCO_3}}\Delta H_{carb}\frac{\partial X_N}{\partial t}-\left[\frac{W_0}{M_{CaCO_3}}C_{p,CaO}(1-X_N)+\frac{W_0}{M_{CaCO_3}}C_{p,CaCO_3}X_N\right]\frac{\partial T}{\partial t}-[C_{p,N_2}Q_g(1-f_{CO_2,in})C_{N_2,in}+C_{p,CO_2}Q_gf_{CO_2,in}C_{CO_2,in}](T-T_{gas,in})-hA(T-T_W)=0 \quad (19)$$

The energy balance for the calcination process with limestone can be written as

$$\frac{W_0}{M_{CaCO_3}}\Delta H_{calci}\frac{\partial X_{CO_2,exit}}{\partial t}+\left[\frac{W_0}{M_{CaCO_3}}C_{p,CaO}(1-f_a)+f_a\frac{W_0}{M_{CaCO_3}}C_{p,CaCO_3}\right]\frac{\partial T}{\partial t}+[C_{p,N_2}Q_g(1-f_{CO_2,in})C_{N_2,in}+C_{p,CO_2}Q_gf_{CO_2,in}C_{CO_2,in}](T-T_{gas,in})+hA(T-T_W)=0 \quad (20)$$

Equations 9 and 10 were solved with eqs 19 and 20 simultaneously with the boundary conditions

$$C_{b,CO_2}=C_{e,CO_2}=C_{CO_2,in} \quad \text{at } z=0 \quad (21)$$

Then, the overall conversion of CO_2 at the reactor exit is

$$X_{CO_2,exit}=1-\frac{\delta u_b^*C_{b,CO_2,exit}+(1-\delta)u_{mf}C_{e,CO_2,exit}}{u_0C_{CO_2,in}} \quad (22)$$

The change of the average carbonation conversion of CaO in the bed can be expressed as

$$X_N=\frac{M_{CaCO_3}}{W_0}\int_0^t Q_g(C_{CO_2,in}-C_{CO_2,exit})dt \quad (23)$$

In addition, the change of the average calcination conversion of $CaCO_3$ in the bed can be expressed as

$$X_{calci}=\frac{M_{CaCO_3}}{X_{u,N}W_0}\int_0^t Q_g(C_{CO_2,exit}-C_{CO_2,in})dt \quad (24)$$

where M_{CaCO_3} is the molecular weight of $CaCO_3$, in 0.1 kg/mol, N is the number of calcination/carbonation cycles, Q_g is the total gas flow entering the bed, in m^3/s, and W_0 is mass of sorbent loaded in the bed, in kg.

The reaction rate constant, K_r, for the carbonation and calcination reactions was defined by incorporating the TGA results to KL models. The reaction rate, K_r, in eqs 9 and 10 for the carbonation reaction and calcination reaction was expressed as

$$K_r=k_c\left(1-\frac{X_N}{X_{u,N}}\right)^m\frac{\rho_{CaO}}{M_{CaO}} \quad \text{for the carbonation stage} \quad (25)$$

$$K_r=k_{calci}(1-X_{calci})^{2/3}\frac{\rho_{CaCO_3}}{M_{CaCO_3}} \quad \text{for the calcination stage} \quad (26)$$

4. Results and Discussion

4.1. Carbonation Results and Discussion. The variations of the CO_2 concentrations with carbonation time for the limestone and dolomite during the CO_2 capture tests for different cycles are shown in Figures 5 and 6, respectively. Both the limestone and dolomite react with CO_2 in two stages. The initial carbonation stage is kinetically controlled with a fast reaction

(18) Kunii, D.; Levenspiel, O. *Ind. Eng. Chem. Res.* **1990**, *29* (7), 1226–1234.

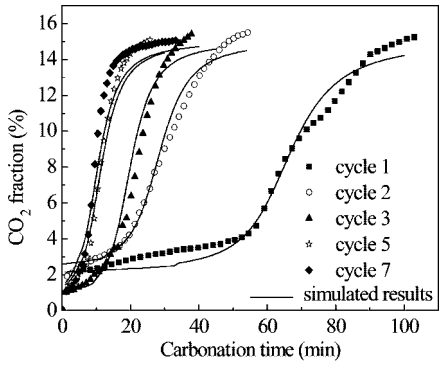

Figure 5. CO_2 concentrations for different cycles during CO_2 capture tests for limestone.

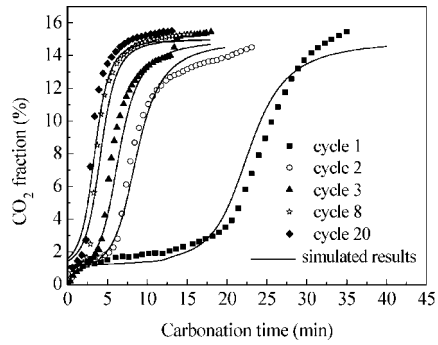

Figure 6. CO_2 concentrations for different cycles during CO_2 capture tests for dolomite.

rate between CaO and CO_2. At this stage, the outlet CO_2 concentrations are not higher than 3% for a stable absorption period. The experimental results of the kinetically controlled stage show that CO_2 in the flue gases can be effectively absorbed by both sorbents in the bubbling fluidized bed. After the stable absorption period, CO_2 concentrations abruptly increased and then increased very slowly, indicating that the CO_2 capture capacity of the CaO was nearly exhausted. It is because that large part of active CaO was converted to $CaCO_3$ and the carbonation stage moved to the second stage controlled by the diffusion in the product layer. Figures 5 and 6 showed that the duration of the effective absorption period (CO_2 concentrations not higher than 3%) decreased as the number of cycles increased because of the loss of CO_2 capture capacity. Abanades et al.[12] reported that the maximum carbonation conversion decreased during the carbonation/calcination cycles because of the loss in the porosity associated with the small pores and the increase in the porosity associated with the large pores.

Figures 5 and 6 also show that the simulated CO_2 concentration profiles in the fluidized bed carbonator calculated with eqs 9, 10, and 19 agree reasonably with the experimental results. The bubble diameter, d_b, strongly influences the simulated results. Larger bubble diameters with the same superficial gas velocity reduce the contact area between the flue gases and sorbent, which reduce the gas conversion. Then, the simulated CO_2 concentrations would be higher than the experiment measured. Conversely, the simulated CO_2 concentration would be lower than the experimental results when the bubble diameters in the KL model are smaller than the actual ones. However, it is almost impossible to determine the bubble size, except by experimental measurement, because so many factors will affect the size, such as the type of distributor of the bed, the fraction of fines in the solid mixture, and the solid properties, especially the density, etc.[21] Therefore, in practical applications, we should measure the bubble diameter experimentally. Typical

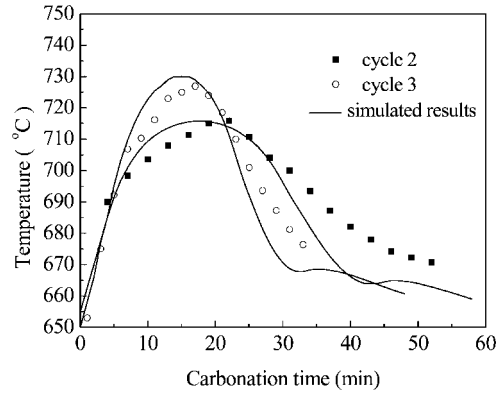

Figure 7. Temperatures versus time for different cycles during CO_2 capture tests for limestone.

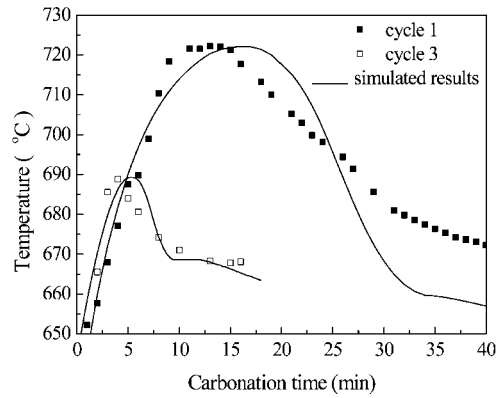

Figure 8. Temperatures versus time for different cycles during CO_2 capture tests for dolomite.

traces of the carbonation temperature in the fluidized bed reactor are compared to the simulated temperature for limestone and dolomite during the different carbonation processes in Figures 7 and 8. The temperatures in the fluidized bed reactor initially increased during the carbonation tests because the reaction of CaO with CO_2 was fast and exothermic. At the end of the kinetically controlled stage, the active CaO was nearly exhausted and the temperatures reached the maximum. Then, the reaction rate of CaO with CO_2 slowed, and the temperatures decreased. The temperature of limestone cycle 2 was not very high because the temperature outside the fluidized bed was only ~620 °C.

4.2. Calcination Results and Discussion. After the CO_2 capture tests, the Ca-based sorbents need regenerating to be used for subsequent cycles. We waited for 10−20 min after the carbonation reaction reached the diffusion-controlled stage. Then, a new CO_2/N_2 ratio (90/10%) flow was introduced into the reactor. When the CO_2 concentration from the online gas analyzer was close to the inlet concentration, the reactor temperature was adjusted to 950 °C and kept stable for some time to completely regenerate the $CaCO_3$ and reactivate the sorbent. As the CO_2 concentration from the online gas analyzer again approached the inlet concentration, the $CaCO_3$ decomposition process was considered finished and the reactor temperature was again cooled to 650 °C and kept stable for some time. Then, the flow rate of the carbonation mixed gas (16% CO_2/84% N_2) was feed into the reactor to continue the carbonation process.

Figures 9 and 10 show the CO_2 fractions and temperatures during the regeneration period as a function of time for different

(19) Baker, E. H. *J. Chem. Soc.* **1962**, *70*, 464–470.
(20) Kunii, D.; Levenspiel, O. *Fluidization Engineering*; Butterworth-Heinemann Press: Oxford, U.K., 1990.
(21) Levenspiel, O. *Ind. Eng. Chem. Res.* **2008**, *47* (2), 273–277.

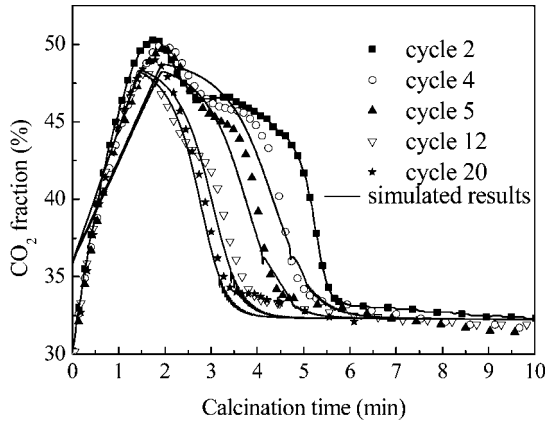

Figure 9. CO_2 concentrations for multiple cycles during regeneration for dolomite.

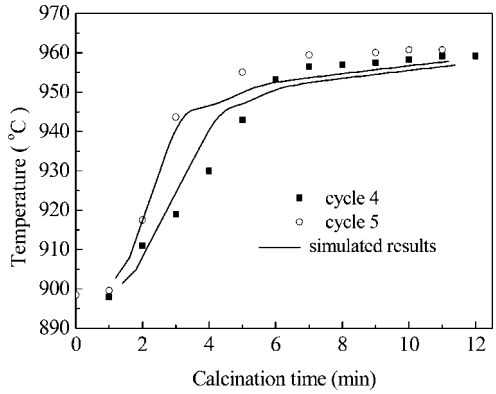

Figure 10. Temperatures in the fourth and fifth cycles during regeneration for dolomite.

cycles of dolomite. Practical applications have two reactors (carbonator and regenerator), with the regenerator keeping the temperature as high as 950 °C. The sorbent circulating from the carbonator to the regenerator was heated quickly from 650 to 950 °C and decomposed back to CaO and CO_2 at the highest rate, consistent with eqs 7 and 8. Therefore, in practical continuous carbonation and calcination systems, the CO_2 concentration at the regenerator exit would remain constant because the regenerator temperature was kept at 950 °C and the sorbent circulation rate was constant. However, in this study, the reactor temperature was gradually raised to 950 °C from 650 °C during the regeneration period because the tests used only one fluidized bed reactor. The heat was provided by an electric furnace, with some time needed for the furnace temperature wall, T_W, to increase from 650 to 950 °C. Then, more time was needed for the reactor temperature to increase from 650 to 950 °C. Therefore, the calcination rate was controlled by the heat transfer in the batch fluidized bed experiment, with the heat transfer greatly influencing the experimental and simulated results. From eq 3, $CaCO_3$ would not decompose until the reactor temperature reached 900 °C. When the temperature in the reactor reached 900 °C, $CaCO_3$ began to decompose and the $CaCO_3$ calcination rate increased with an increasing reactor temperature, consistent with eqs 7 and 8, resulting in the CO_2 fraction gradually increasing with time as seen in Figures 9 and 10. When the reactor temperature approached 950 °C, the $CaCO_3$ decomposition rate was accelerated greatly and the CO_2 fraction approached the maximum. With the increase of the regeneration time, the fraction of unreacted $CaCO_3$ in the reactor and the CO_2 fraction at the reactor exit began to decrease with time. When all of the $CaCO_3$ was calcined, no CO_2 was released from the sorbent and the CO_2 concentration approached the inlet level. The energy balance for the calcination process in eq 20 and the apparent kinetic model in eqs 7 and 8 indicate that, if the heat-transfer rate is increased, the maximum CO_2 concentration will appear earlier. Figures 9 and 10 show that the simulated results agree well with the experimental data for the calcination steps. The duration of the regeneration step and the total amount of CO_2 released decreased with an increasing number of cycles. Figure 9 can also be used to determine the CO_2 capture capacity by integrating the CO_2 released over time.

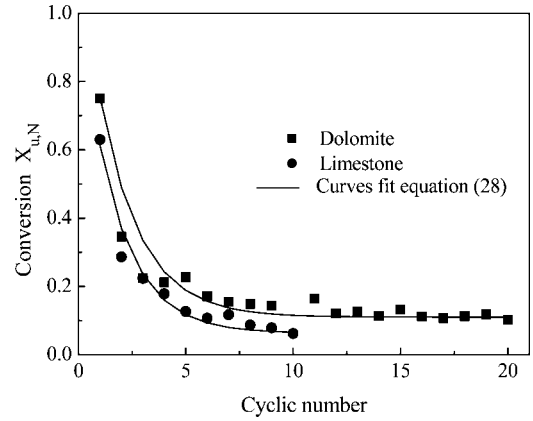

Figure 11. Sorbent cyclic conversion reduction.

4.3. Sorbent Activity Decrease. The conversion of CaO to $CaCO_3$ in the carbonation step decreases with an increasing number of cycles of carbonation/calcination.[10,12] Recently, Grasa et al.[22] tested a long series of carbonation/calcination cycles (up to 500 cycles) and found that the residual conversion of about 7−8% remained constant after hundreds of cycles and seemed insensitive to process conditions.

Abanades[23] studied the experimental data on repeated CaO carbonation/calcination cycles for various conditions and found that the decrease in the conversion was only dependent upon the number of cycles and could be described by

$$X_{u,N} = f^{N+1} + b \tag{27}$$

This work used a semi-empirical equation to describe the conversion reduction with the number of cycles based on the current data

$$X_{u,N} = af^{N+1} + b \tag{28}$$

where a, b, and f are constants. Equation 28 describes the conversion decrease of limestone and dolomite sorbents with different a, b, and f for the different sorbents determined from fitting the experimental results. The CO_2 capture capacity can be determined from either the CO_2 response curves during the CO_2 capture or the regeneration tests, with these two values showing good agreement. In this study, the carbonation values were used to calculate the CO_2 capture capacity shown in Figure 11. The solid lines are the best-fit curves to eq 28 for limestone ($a = 1.75$, $b = 0.063$, and $f = 0.56$) and dolomite ($a = 1.85$, $b = 0.11$, and $f = 0.59$). Figure 11 shows that, at first, with an increasing number of carbonation/calcination cycles, $X_{u,N}$ decreased continuously because of the decrease of CaO activity. The decline of the CO_2 capture capacity with an increasing number of carbonation/calcination cycles can be attributed to changes in the structural properties of the sorbent during

(22) Grasa, G. S.; Abanades, J. C. *Ind. Eng. Chem. Res.* **2006**, *45*, 8846–8851.
(23) Abanades, J. C. *Chem. Eng. J.* **2002**, *90*, 303–308.

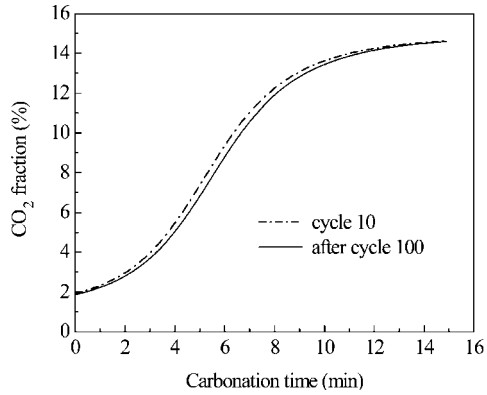

Figure 12. Carbonation of 10 and 100 cycles predicted by the KL model and eq 28.

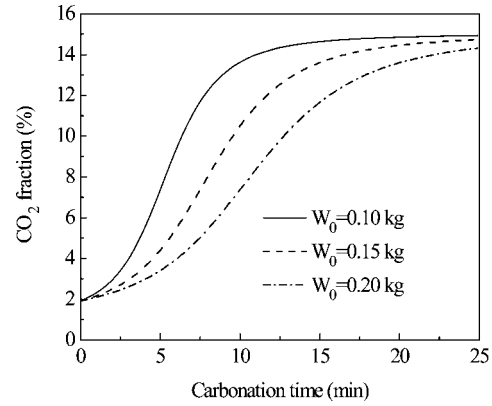

Figure 13. Predicted effect of limestone sorbent mass in the reactor on the CO_2 capture process after many cycles ($X_{u,N} = 0.063$).

calcination.[24] After the reaction of CaO with CO_2, the product $CaCO_3$ must undergo calcination to regenerate CaO for repeated used. In the calcination process, some pores are produced inside the CaO particle but, at the same time, CaO sintering occurs because of the high calcination temperature, which reduces the surface area and porosity with an increasing residence time. The surface area and porosity are very important for the reaction of CaO with CO_2, but sintering sharply reduces surface area and porosity, which strongly affects the CO_2 capture capacity and the reaction rates of CaO with CO_2. As the number of carbonation/calcination cycles for limestone and dolomite exceeds about 10 cycles, $X_{u,N}$ no longer decreases because both sorbents already approach their lowest ultimate conversion. Figure 11 shows a similar decrease of CO_2 capture capacity of limestone and dolomite, which differ from previous studies that indicated that dolomite had better cyclic capacity of capturing CO_2.[11,22] The high melting point compounds, such as MgO in the Ca-based sorbent, may inhibit sintering to some extent but will not completely eliminate sintering. The high calcination temperature (950 °C) and CO_2 fraction (>90%) in the present study were higher than previous studies,[11,22] and this may have accelerated the sintering. Thus, MgO will have little effect on decreasing sintering under the severe conditions. Therefore, the dolomite has a similar decrease of capacity as limestone under severe conditions.

From a practical point of view, in continuous carbonation/calcination systems, the sorbents must be used repeatedly and the value of $X_{u,N}$ should be kept low to maximize use of the sorbent and minimize the loss of active CaO. The carbonation of limestone at the 10th cycle and after 100 cycles can be predicted by the KL model using eq 28, as shown in Figure 12. The final carbonation conversion, $X_{u,N}$, of the 10th cycle is 0.066, and $X_{u,N}$ is 0.063 after the 100th cycle without change. As can be seen from Figure 12, the residual active CaO in the fluidized bed reactor after many cycles still captures CO_2 from the combustion flue gas at high temperatures, with the carbonation characteristics having neglectable differences after many cycles, because the sorbent has reaches its lowest ultimate conversion. For stable values of $X_{u,N}$ (0.063), the mass of sorbent in the bed strongly affects the CO_2 capture efficiency in the gas phase as shown in Figure 13. The length of the stable CO_2 capture stage became shorter as the total sorbent mass, W_0, was reduced, with the abrupt increase in the CO_2 concentration occurring earlier.

4.4. Prediction of CO_2 Capture in a Continuous Carbonation and Calcination System. Carbonation/calcination cycles with Ca-based sorbents to capture CO_2 in flue gases consist of dual fluidized bed reactors with one as the carbonator and the other as the regenerator, as shown in Figure 1. In continuous cycles, the sorbent alternates between these two reactors by solid transport lines. However, the capacity of the Ca-based sorbents for capturing CO_2 decreases with an increasing number of cycles; therefore, the makeup of fresh sorbent is required to maintain a high CO_2 capture. According to the sorbent activity loss, the carbonation kinetic rate also decreases with the number of cycles, which is important for the determination of sorbent inventory in the carbonator and the reactor structure. When dual fluidized bed reactors are used for the carbonation and calcination cycles, the solid sorbent circulation between two reactors is critical and the sorbent reactivity loss, carbonation kinetic rates, and gas velocity have significant effects on the reactor structure. All of these variants should be considered in designing reactors.

Table 1. Parameters for the Prediction of CO_2 Capture

	A_{abs}	T	u_0	d_b
	973 m^2	650 °C	1.35 m/s	0.068 m
flow	CO_2 (kmol/s)	O_2 (kmol/s)	N_2 (kmol/s)	H_2O (kmol/s)
inlet	2.91	0.65	14.73	1.26
outlet	0.49	0.65	14.73	1.26

4.4.1. Mass Balance. For the process shown in Figure 1, the molar flow rate of fresh sorbent is F_0 (kmol/s). To maintain a fixed amount of material in the system, the same amount of spent sorbent [F_0 (kmol/s)] must be discharged. F_R (kmol/s) is the sorbent molar flow rate from the carbonator to the regenerator. $F_R + F_0$ is the solid molar flow rate from the regenerator to the carbonator.[25]

Assuming complete mixing of the sorbent in the system, there are sorbents undergoing $1-N$ cycles in both the carbonator and regenerator. The mass fraction, r_N, of the sorbent entering the carbonator is[23]

$$r_N = \frac{F_0 F_R^{N-1}}{(F_0 + F_R)^N} \tag{29}$$

When the sorbent is recycled between the carbonator and regenerator, the average CaO conversion in the carbonator is[23]

$$X_{abs} = \sum_{N=1}^{N=\infty} \frac{F_0 F_R^{N-1}}{(F_0 + F_R)^N} X_{u,N} \tag{30}$$

(24) Silaban, A.; Harrison, P. *Chem. Eng. Commun.* **1995**, *137*, 177–190.
(25) Li, Z.-S.; Cai, N.-S.; Eric, C. *AIChE J.* **2008**, *54* (7), 1912–1925.
(26) Alberto, A.; Juan, A.; Francisco, G. L.; Luis, F. D.; Pilar, G.; Javier, C. *Chem. Eng. Sci.* **2007**, *62*, 533–549.

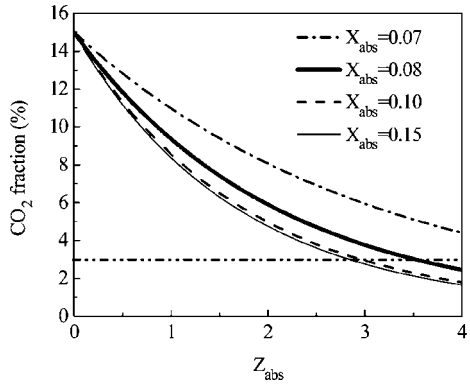

Figure 14. Predictive CO_2 fractions with the bed height of carbonator for various average conversions.

After incorporating eq 28 into eq 30, the limit of the infinite sum of the geometric series is

$$X_{abs} = \frac{afF_0}{F_0 + F_R(1-f)} + b \tag{31}$$

The mass balance in Figure 1 is

$$(F_R + F_0)\Delta X = F_{CO_2} \tag{32}$$

$$\Delta X = X_{abs} - X_{reg} \tag{33}$$

The following assumes that the $CaCO_3$ decomposes completely in the regenerator; therefore, X_{reg} is equal to zero and $\Delta X = X_{abs}$.[25]

τ_{abs} is the average solid residence time in the carbonator calculated from the molar flow rate of the solid, $F_R + F_0$, and the total molar of the solid in the bed, F_{abs}, as

$$\tau_{abs} = \frac{F_{abs}}{F_0 + F_R} = \frac{A_{abs}Z_{abs}(1-\varepsilon_f)C_{abs}}{F_0 + F_R} \tag{34}$$

4.4.2. Average Carbonation Reaction Rate. Because the sorbent is continuously exchanged between the two reactors, the sorbents, which have circulated N times, have different residence times in the carbonation reactor. Therefore, the average carbonation reaction rate of the sorbent circulating N times in the carbonation/calcination cycles is

$$\frac{d\bar{X}_N}{dt} = \int_0^\tau \frac{dX_N}{dt} E(t)dt \tag{35}$$

where the exit age distribution for the solids in the carbonator is

$$E(t) = \frac{1}{\tau_{abs}} \exp\left(-\frac{\tau}{\tau_{abs}}\right) \tag{36}$$

In the practical CCR process, for maintaining the low CO_2 concentration at the carbonator exit, we mainly use the kinetically controlled stage in the carbonation process; therefore, m in eq 5 is taken $^2/_3$. After some manipulation, eq 5 can be written as

$$\frac{dX_N}{dt} = k_c X_{u,N}^{-2/3}(\bar{C} - C_{eq,CO_2})\left[X_{u,N}^{1/3} - \frac{1}{3}k_c X_{u,N}^{-2/3}(\bar{C} - C_{eq,CO_2})t\right]^2 \tag{37}$$

Incorporation of eqs 36 and 37 into eq 35 gives

$$\frac{d\bar{X}_N}{dt} = \int_{t=0}^{t=\tau} k_c X_{u,N}^{-2/3}(\bar{C} - C_{eq,CO_2})\left[X_{u,N}^{1/3} - \frac{1}{3}k_c X_{u,N}^{-2/3}(\bar{C} - C_{eq,CO_2})t\right]^2 \frac{e^{-t/\tau_{abs}}}{\tau_{abs}}dt = \lambda_{abs}(\bar{C} - C_{eq,CO_2}) \tag{38}$$

where

$$a_{abs} = \frac{1}{3}k_c X_{u,N}^{-2/3}(\bar{C} - C_{eq,CO_2}) \tag{39}$$

$$\lambda_{abs} = k_c X_{u,N}^{-2/3}\{X_{u,N}^{2/3} - (X_{u,N}^{1/3} - a_{abs}\tau)^2 e^{\tau/\tau_{abs}} - 2a_{abs}\tau_{abs}[X_{u,N}^{1/3} - (X_{u,N}^{1/3} - a_{abs}\tau)e^{\tau/\tau_{abs}}] + 2(a_{abs}\tau_{abs})^2(1 - e^{\tau/\tau_{abs}})\} \tag{40}$$

The average concentration of the reacting gas, $\bar{C}$, is[26]

$$\bar{C} = \frac{\Delta X_g C_{CO_2,in}}{\int_{X_{g,in}}^{X_{g,out}} \frac{1+\varepsilon_g X_g}{1-X_g} dX_g} \tag{41}$$

$$\varepsilon_g = \frac{V_{g,X_g=1} - V_{g,X_g=0}}{V_{g,X_g=0}} \tag{42}$$

where X_g is the gas conversion and ε_g is the coefficient of expansion of the gas mixture, which is equal to -0.15 in this work.

There are sorbents undergoing $1-N$ cycles in the carbonator; therefore, the average carbonation rate is

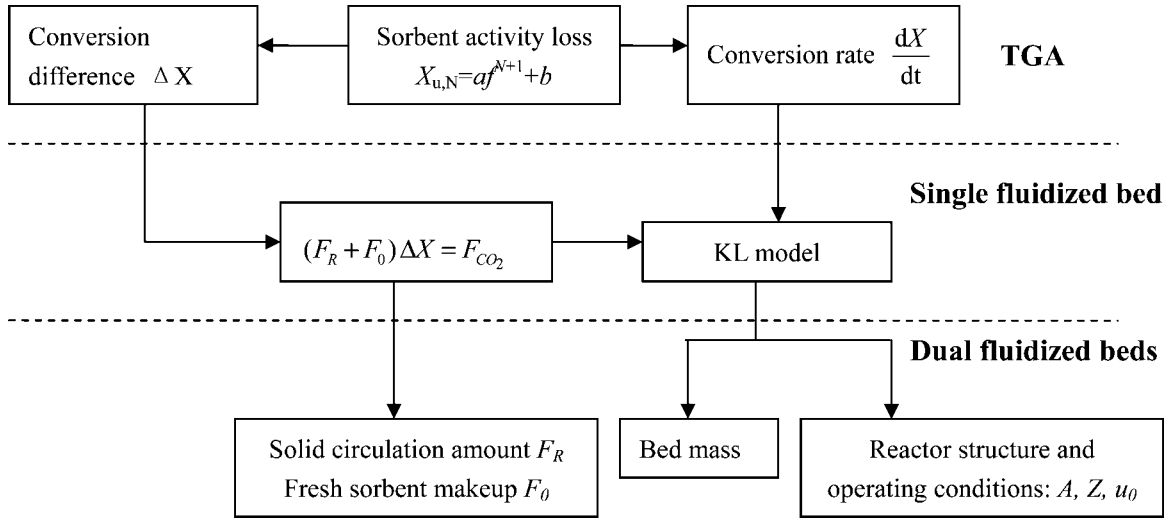

Figure 15. Research and design consideration of the CCR process.

$$\frac{dX_{ave}}{dt} = \sum_{N=1}^{N=\infty} \frac{F_0 F_R^{N-1}}{(F_0 + F_R)^N} \frac{d\bar{X}_N}{dt} = \sum_{N=1}^{N=\infty} \frac{F_0 F_R^{N-1}}{(F_0 + F_R)^N} \lambda_{abs}(\bar{C} - C_{eq,CO_2}) \quad (43)$$

Therefore, the reaction rate, K_r, is

$$K_r = \frac{\rho_{CaO}}{M_{CaO}} \sum_{N=1}^{N=\infty} \frac{F_0 F_R^{N-1}}{(F_0 + F_R)^N} \lambda_{abs} \quad (44)$$

4.4.3. Predictive Results of CO_2 Capture in a Continuous Carbonation and Calcination System. Equation 43 can be used in the KL model to simulate the CO_2 capture in a continuous carbonation and calcination system. The molar flow rates of flue gas from the coal-fired power plant and the carbonator structure[5] and the carbonator temperature are listed in Table 1, where Z_{abs} is assumed to be 4 *m*. Limestone is used as a CO_2 sorbent and is regenerated under the severe calcination conditions (950 °C calcination temperature and >90 vol % CO_2 atmosphere) in the regenerator.

The profile of the average CO_2 concentration with bed height is shown in Figure 14. If the exit CO_2 concentration is below 3%, about 83% of the CO_2 is absorbed by the sorbent in the carbonator. From Figure 14, as the average CaO conversion, X_{abs}, in the carbonator increases, the CO_2 removal efficiency improves. For an average conversion, X_{abs}, of 0.08, ~86% of the CO_2 was captured at the carbonator exit. The addition of more fresh sorbent into the system gave an average CaO conversion of 0.15, and approximately, 90% of the CO_2 was captured at the carbonator exit. For X_{abs} equal to 0.15, the amount of fresh sorbent (F_0) added was 0.6379 kmol/s, while for X_{abs} equal to 0.08, the amount of fresh sorbent (F_0) added was 0.2243 kmol/s. Thus, the amount of fresh sorbent (F_0) for X_{abs} equal to 0.15 was 2.84 times as much as for X_{abs} equal to 0.08.

4.5. Integration of TGA and Single and Dual Fluidized Bed Reactors. Previous studies focused on the sorbent activity decrease[10−15] or kinetic models of the CCR process in a TGA[27] or single fluidized bed[13] alone. However, there has been neither a clear connection among these studies nor a system that can link the sorbent activity decrease and the kinetic models of the CCR process in a TGA and single fluidized bed reactor to the design of dual fluidized bed reactors.

Figure 15 shows the research and design ideas of the CCR process, from which a clear and integrated research plan can be derived. The TGA experiments give an equation describing the sorbent activity and the conversion rate d*X*/d*t* for multiple cycles. The TGA research results of sorbent activity can be used to determine the mass balance of the CCR process and then to determine the fresh sorbent rate, F_0, and the solid circulation rate, F_R. Integrating the sorbent activity loss, conversion rate, and mass balance, the KL model is developed and validated with single fluidized bed experimental data. Finally, the KL model can be used to predict the CO_2 capture in continuous carbonation and calcination system to determine the bed inventory mass and reactor structure and operation conditions, which can give useful information to the design and operation of reactors for the CCR process.

5. Conclusions

CO_2 fractions and temperatures for multiple cycles of carbonation/calcination reactions of limestone and dolomite were measured experimentally with a simple bubbling bed model (KL model) developed to describe the process. The model was used to predict the variations of the CO_2 concentration and temperature profiles with time in multiple carbonation and calcination reactions. The model results qualitatively agree with the experimental data and delineate important features of the system. The stable absorption time initially decreases because of the loss of the sorbent activity with the increasing number of cycles for limestone and dolomite and then remains nearly constant with more cycles, because the sorbent has already reached its final residual capture capacity. $CaCO_3$ decomposition in a fluidized bed reactor is affected by the CO_2 partial pressure, calcination temperature, and heat-transfer rate; therefore, these parameters should be determined on the basis of the required sorbent regeneration step in the practical process. In a continuous carbonation/calcination system, the sorbent activity loss influences the circulation rate between two reactors and average carbonation rate; the mass balance and average carbonation rate influence the reactor structures. On the basis of the KL model, the CO_2 capture in a continuous carbonation/calcination system was predicted considering the mass balance, sorbent circulation rate, sorbent activity loss, and the average carbonation kinetic rates to give useful information to the design and operation of reactors for the CCR process.

Acknowledgment. This work was supported by the National Basic Research Program of China (2006CB705807) and the National Natural Science Funds of China (No. 50806038).

Nomenclature

A = heat exchange surface area, m^2
A_{abs} = area carbonator cross-sectional, m^2
$\bar{C}$ = average concentration of reacting gas, mol/m^3
C_{abs} = average concentration of sorbent in the carbonator, $kmol/m^3$
C_{b,CO_2} = CO_2 concentration in the gas bubble phase, mol/m^3
C_{e,CO_2} = CO_2 concentration in the emulsion phase, mol/m^3
C_{eq,CO_2} = equilibrium concentration of CO_2 over CaO, mol/m^3
$C_{b,CO_2,exit}$ = CO_2 concentration in the gas bubble phase at the reactor exit, mol/m^3
$C_{e,CO_2,exit}$ = CO_2 concentration in the emulsion phase at the reactor exit, mol/m^3
$C_{CO_2,exit}$ = total CO_2 concentration at the reactor exit, mol/m^3
$C_{CO_2,in}$ = total CO_2 concentration at the reactor entrance, mol/m^3
$C_{N_2,in}$ = total N_2 concentration at the reactor entrance, mol/m^3
$C_{p,CaO}$ = heat capacity of CaO, $J\ K^{-1}\ mol^{-1}$
$C_{p,CaCO_3}$ = heat capacity of $CaCO_3$, $J\ K^{-1}\ mol^{-1}$
C_{p,N_2} = heat capacity of N_2, $J\ K^{-1}\ mol^{-1}$
C_{p,CO_2} = heat capacity of CO_2, $J\ K^{-1}\ mol^{-1}$
d_b = effective bubble diameter, m
d_p = particle diameter, m
F_0 = molar flow rate of fresh sorbent, kmol/s
F_R = sorbent molar flow rate from the carbonator to the regenerator, kmol/s
f_a = fraction of active CaO in the carbonation process or fraction of nonreacting $CaCO_3$ to the sorbent in the calcination process
$f_{CO_2,in}$ = bulk fraction of CO_2 in the inlet gas
g = acceleration of gravity, $9.8\ m/s^2$
ΔH_{calci} = heat of reaction for the calcination endothermic reaction
ΔH_{carb} = heat of reaction for the carbonation exothermic reaction
h = heat-transfer coefficient, $W\ m^{-2}\ K^{-1}$
K_{be} = overall gas interchange coefficient between bubble and emulsion phases, s^{-1}
K_r = rate constant for a first-order reaction, s^{-1}
k_{calci} = chemical rate constant in the calcination process, $m^3\ mol^{-1}\ s^{-1}$
$k_{0,calci}$ = effective reaction rate constant in eq 14
k_c = chemical rate constant for the gas−solid reaction in the carbonation process, $m^3\ mol^{-1}\ s^{-1}$
M_{CaCO_3} = molecular weight of $CaCO_3$, 0.1 kg/mol

(27) Lee, D. K. *Chem. Eng. J.* **2004**, *100*, 71–77.

m = effective constant in eq 12
N = cycle number
Q_g = total gas flow entering the bed, m^3/s
R = gas constant, J mol^{-1} K^{-1}
r_N = mass fraction of sorbents entering the carbonator
T = reactor temperature, K
T_W = furnace wall temperature, K
$T_{gas,in}$ = gas temperature entering the reactor, K
t = time, s
u_{mf} = superficial gas velocity at the minimum fluidizing conditions, m/s
u_0 = superficial gas velocity, m/s
u_b = velocity of a bubble rising through a bed, m/s
u_b^* = rise velocity of bubble gas, m/s
V_g = gas mixture volume, m^3
W_0 = mass of sorbent loaded in the bed, kg
X_{abs} = average CaO conversion in the carbonator
X_{calci} = calcination conversion in the bed
X_b = reaction gas conversion
X_r = final conversion after many cycles
X_N = carbonation conversion in the bed
X_{reg} = average CaO conversion in the regenerator
$X_{u,N}$ = final carbonation conversion in the bed at the Nth cycle
Z_{abs} = carbonator height, m
z = height of solids loaded in the bed under bubbling condition, m
γ_b = volume of solids dispersed in bubbles
δ = bubble fraction in the bed
ε_{mf} = void fraction in the bed at minimum fluidized conditions
ε_f = void fraction in the fluidized bed, $\delta + (1 - \delta)\varepsilon_{mf}$
ε_g = coefficient of expansion of the gas mixture
μ = gas viscosity, kg m^{-1} s^{-1}
ρ_s = solid density, kg/m^3
ρ_g = gas density, kg/m^3
ϕ_s = sphericity of the sorbent
τ_{abs} = average solid residence time during carbonation, s

EF800474N